AD-A158 321 NOVEL TRANSPORT AND RECOMBINATION PROCESSES IN SEMICONDUCTORS(U) CAMBRIDGE UNIV (ENGLAND) CAVENDISH LAB M PEPPER MAR 85 DAJA37-82-C-0181 1/1

UNCLASSIFIED F/G 20/12 NL

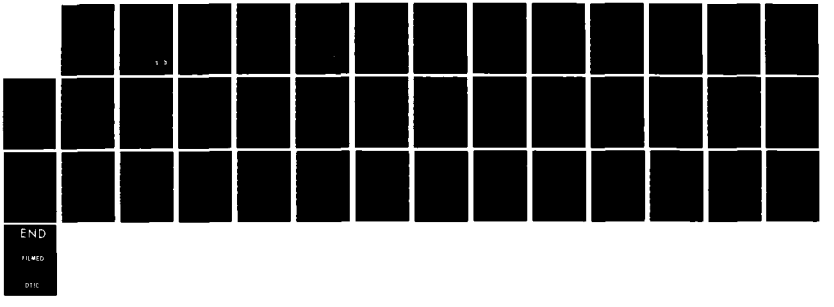

END

FILMED

DTIC

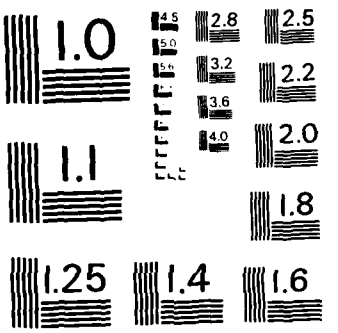

R+D-4072 (2)

NOVEL TRANSPORT AND RECOMBINATION PROCESSES IN SEMICONDUCTORS

FINAL TECHNICAL REPORT

by

M. PEPPER

MARCH 1985

EUROPEAN RESEARCH OFFICE

United States Army

London England

CONTRACT NUMBER DAJA37-82-C-0181

GR: Cavendish Laboratory
Department of Physics
University of Cambridge
Cambridge
CB3 0HE
U.K.

Approved for Public Release: distribution unlimited

UNCLASSIFIED
SECURITY CLASSIFICATION OF THIS PAGE (When Data Entered)

R&D 4072-EE

REPORT DOCUMENTATION PAGE	READ INSTRUCTIONS BEFORE COMPLETING FORM
1. REPORT NUMBER	2. GOVT ACCESSION NO. AD-A158321 / 3. RECIPIENT'S CATALOG NUMBER
4. TITLE (and Subtitle) Novel Transport and Recombination Processes in Semiconductors	5. TYPE OF REPORT & PERIOD COVERED Final Technical Report Mar 82 - Jun 85
	6. PERFORMING ORG. REPORT NUMBER
7. AUTHOR(s) M. Pepper	8. CONTRACT OR GRANT NUMBER(s) DAJA37-82-C-0181
9. PERFORMING ORGANIZATION NAME AND ADDRESS Cavendish Laboratory University of Cambridge Cambridge, UK	10. PROGRAM ELEMENT, PROJECT, TASK AREA & WORK UNIT NUMBERS 61102A 1T161102BH57-03
11. CONTROLLING OFFICE NAME AND ADDRESS USARDSG-UK Box 65, FPO NY 09510-1500	12. REPORT DATE March 1985
	13. NUMBER OF PAGES 37
14. MONITORING AGENCY NAME & ADDRESS(if different from Controlling Office)	15. SECURITY CLASS. (of this report) Unclassified
	15a. DECLASSIFICATION/DOWNGRADING SCHEDULE

16. DISTRIBUTION STATEMENT (of this Report)

Approved for Public Release; distribution unlimited

17. DISTRIBUTION STATEMENT (of the abstract entered in Block 20, if different from Report)

18. SUPPLEMENTARY NOTES

19. KEY WORDS (Continue on reverse side if necessary and identify by block number)

SPIN, RECOMBINATION, LOCALISATION, QUANTUM HALL EFFECT, BALLISTIC TRANSPORT, PLASMONS.

20. ABSTRACT (Continue on reverse side if necessary and identify by block number)

This report describes work on spin dependent recombination processes, electron injection from point contacts into semiconductors and the Quantisation of Hall resistance in strong magnetic fields.

The work on spin dependent processes has identified spin dependent recombination and generation processes as well as a non-resonant magnetic field effect centred at zero magnetic field. This effect clearly has the same cause as the

DD FORM 1 JAN 73 1473 EDITION OF 1 NOV 65 IS OBSOLETE

UNCLASSIFIED
SECURITY CLASSIFICATION OF THIS PAGE (When Data Entered)

resonant generation and recombination processes. Resonance effects were constant over a wide range of frequencies confirming theoretical predictions that this was the case.

Work on two dimensional systems has concentrated on the two terminal properties in the regime of quantised Hall resistance. The inversion layer has been shown to behave as a voltage source with quantised impedance. Frequency measurements have shown that fractional quantisation can be introduced as integer quantisation is destroyed. The frequency dependence is shown to be dependent on sample length, this being the maximum localisation length which can occur.

Point contact injection from Al and Ag point contacts into Si has been investigated, it is shown that instabilities occur due to coupling between electrons and plasmons.

ABSTRACT

This report describes work on spin dependent recombination processes, electron injection from point contacts into semiconductors and the Quantisation of Hall resistance in strong magnetic fields.

The work on spin dependent processes has identified spin dependent recombination and generation processes as well as a non-resonant magnetic field effect centred at zero magnetic field. This effect clearly has the same cause as the resonant generation and recombination processes. Resonance effects were constant over a wide range of frequencies confirming theoretical predictions that this was the case.

[illegible]on two dimensional systems has concentrated on the two terminal properties in the regime of quantised Hall resistance. The inversion layer has been shown to behave as a voltage source with quantised impedance. Frequency measurements have shown that fractional quantisation can be introduced as integer quantisation is destroyed. The frequency dependence is shown to be dependent on sample length, this being the maximum localisation length which can occur.

Point contact injection from Al and Ag point contacts into Si has been investigated, it is shown that instabilities occur due to coupling between electrons and plasmons.

2. Introduction

We now present the abstracts of preprints and reprints supported by this contract. The complete description of this work is in section 5.

"Non-linearities and electron-plasmon coupling in metal-semiconductor point contacts" P.W.A. McIlroy and M. Pepper, J.Phys C 18, L87, 1985.
Abstract: We have investigated the current-voltage characteristics of Al: Si and Ag: Si point contacts in the region of energy corresponding to plasmon excitation. We present results showing resonant structure in d^2I/dV^2 close to the Al surface plasmon energy and bistable switching close to the Al and Ag surface plasmon energies.

"Two-terminal conductance of the quantised Hall resistor" T.G. Powell, C.C. Dean and M. Pepper", J. Phys C 17, L359, 1985.
Abstract: Two-terminal conductance measurements on a two-dimensional inversion layer are shown to give values ie^2/h when E_F lies between Landau sub-bands. Investigation of conductance with resistive connections across the inversion layer shows opposite contacts to behave as a voltage source with characteristic impedance h/ie^2.

"Frequency dependent magnetoconductance quantisation in 2D systems - a disorder effect". T.G. Powell, R. Newbury, A.P. Long, C. McFadden, H.W. Myron and M. Pepper, J.Phys C, in the press.
Abstract: Strong frequency dependence is shown in the quantised magnetoconductance in high mobility silicon MOSFETS, with the loss of integer quantised plateaux and enhancement of fractional quantisation. Fractional plateaux observed are quantised to within 5%, which is within experimental accuracy. The frequency at which the onset of these phenomena is observed is shown to be dependent upon sample length and Landau level filling factor. The results are similar to those previously obtained using low mobility GaAs heterostructures, though in the highest mobility cases no effect is seen up to 50 MHz. The roles of sample length and disorder are discussed.

3. Publications Supported by this Contract

a. "Non-linearities and electron-plasmon coupling in metal-semiconductor point contacts". P.W.A. McIlroy and M. Pepper, J.Phys C 18, L87, 1985.

b. "Two-terminal conductance of the quantised Hall resistor", T.G. Powell, C.C. Dean and M. Pepper, J.Phys C 17, L359, 1985.

c. "Frequency Induced Electron Delocalisation and Fractional Quantisation In Silicon Inversion Layers", A.P. Long, H.W. Myron and M. Pepper, J.Phys C 17, L433, 1984.

d. "Frequency Enhanced Fractional Quantisation in GaAs-AlGaAs Hetero-junctions", C. McFadden, A.P. Long, H.W. Myron, M. Pepper, G.J. Davies and D. Andrews, J.Phys C 17, L439, 1984.

e. "Frequency Dependent Magnetoconductance Quantisation in 2D systems - a disorder effect", T.G. Powell, R. Newbury, A.P. Long, C. McFadden H.W. Myron and M. Pepper, J.Phys C, in the press.

4. SPIN DEPENDENT EXPERIMENTS WITH SILICON P-n JUNCTIONS

These experiments were carried out in association with Dr. R.L. Vranch, who obtained his Ph.D for research on SDR. In these experiments the enhancement of the recombination current at the resonance condition was investigated using gate controlled p+n junctions. Many experiments were performed using irradiated devices in order to increase the strength of the signal. The irradiation was either from a Co60 Gamma ray source or a 30keV beam of electrons. The principal results of the experiments will now be presented.

1. The determination of the g value

This was determined by comparing the value of magnetic field (B_0) at the centre of a resonance with the value of B_0 at the centre of a DPPH resonance. This latter resonance has a known value of 2.0036, the DPPH resonance was sharp and had a peak-to-peak width of 0.2 milli-Tesla. The DPPH resonance was detected using the device, as the reduction in the microwave induced pick-up voltage caused a change in the device current. Figure 1 shows a DPPH trace and an SDR signal obtained from an irradiated junction, the ascertained g value was 2.0051 ± 0.0002. The relative change in current at resonance was $2.7.10^{-4}$. No signals were detected from unirradiated (100) or (111) orientation devices. A g value of 2.0076 ± 0.0005 was found with a (111) device, this agrees[1] with the value of 2.0081 found for P_b centres on (111) oxidised Si. Signals were also induced by the avalanche injection of holes into the SiO_2 from the Si.

2. Spin Dependent Generation

An SDG signal was found having the same centre field and width as SDR but with opposite phase. This SDG signal appeared to be brought about by the same centres which were responsible for SDR, figure 2. The relative size of the SDG signal was always slightly larger than the size of the corresponding SDR signal. Although the SDG current was an order of magnitude less than SDR, the improvement in the signal-to-noise ratio was much better for SDG and, therefore, this was often measured in preference to SDR.

An investigation of the shape of an SDG signal from an irradiated P channel (111) device revealed small resonances located 2.2 ± 0.3 milli-Tesla on either side of the main SDG resonance, figure 3. These were not found in (100) SDG or SDR, and were strikingly similar to the Si 29 hyperfine signals found with ESR on the (111) surface which confirmed that the defect was a Si dangling bond at the interface.[2]

A key prediction of the model of Kaplan, Solomon and Mott (KSM)[3] used in the interpretation of the experiments is that the size of the signal is independent of the frequency of the microwave signal. In confirmation of this, the signal was found to be the same height and width at 7.0 GHz, 9.45 GHz and 12.0 GHz.

3. The Radio Frequency SDR Signal

The SDR signal was investigated with a radio frequency magnetic field in place of the microwave field. A helical cavity was used which supplied 3 watts of r.f. power at 440 MHz. Figure 4 shows the SDR, SDG and DPPH traces found. The important feature of this result is that the size of the SDR signal is $3.3\ 10^{-4}$ which is about the same as at X band frequencies. This is predicted by the KSM model, but other models based on a spin polarisation predict that the size of the signal varies as B^2 and, hence, the 440 MHz signal should be $\approx 10^{-3}$ of the size of the X band signal. This is clearly contradicted by the experiments.

The lack of a frequency dependence of signal width indicates that the signal comprises electron and hole signals with the same g value. The alternative point of view of different g values would give a field dependent linewidth. This similarity of g values was also indicated by the lack of a spin dephasing effect.

4. The Variation of Diode Biasing

In general SDG signals were easier to interpret since all the current is due to generation. On the other hand, the forward current is due to both generation and recombination and the SDR proportion cannot be established precisely. The lineshapes and g values of signals from irradiated devices were unaffected by variations in junction voltage (V_j) or gate voltage (V_g). This goes with the observation of Poindexter et al that the linewidth of the ESR P_b signal was independent of gate voltage[4]. Depending on the value of V_G the SDR signal strength ($\Delta I/I$) was constant up to junction currents in the range 10^{-7} to 10^{-8} amps. For greater currents the strength fell as the current was increasingly dominated by diffusion. As expected, the enhancement of the generation rate was independent of the size of the generation current and was the same as the recombination enhancement at low values of forward current.

5. Half Field Resonances

On one irradiated device a large signal was found at half the resonance conduction for both 9.454 GHz and 7.092 GHz. The half field resonance was bigger than the normal signal and was not found with other devices. This effect has been observed in other semiconductor systems and is associated with transitions between upper and lower triplet levels. It is surprising that it was observed here.

6. MNOS Devices

These devices had a thin (20Å oxide) interfaced between Si and Si_3N_4. The g values of the signals were always larger than those obtained with MNOS structures. The devices were (111) orientation and the size of the signal varied randomly between devices. SDG signals were found with a g value of 2.010 $\pm$ 0.001 close to the value found by Kaplan et al[5] who measured ESR on wafers treated with nitric acid. This agreement is perhaps not surprising as the oxides in the devices were grown by exposure to nitric acid. The absence of the P_b centre presumably reflects the totally different interfacial structure.

7. Non-Resonance Experiments

Non-resonant signals at zero field were found in the absence of microwaves. The signals were found in generation and recombination and were the same size as the SDR and SDG signals found in the presence of the microwaves. However, the non-resonant signals were wider than the resonant ones, the tails decaying even more slowly than a Lorentzian derivative. Explanations for this effect are not clear but the origin may lie in the dipole-dipole interaction. Figure 5 illustrates the effect of reducing the magnetic field, as seen structure appears at B=0 indicating the existence of two closely separated resonances.

Summary

The g values of the SDR signals indicated that the coupled dangling bonds responsible for trapping and the SDR signal are the ESR P_b centres. This is consistent with the recent identification by Poindexter et al[1,4] of the P_b centre as the interface defect responsible for the peak in the upper and lower halves of the band gap in unannealed oxidised silicon. The resonant signal corresponds to singlet-triplet transitions but the role of the half-field resonance is not clear. A novel feature of this work was the observation of the non-resonant spin dependent effects at zero field. This has been found in other systems and the explanations have been in terms of the relaxation of trapped triplet state electron-hole pairs. It is not clear if this explanation is applicable to the Si-SiO_2 interface. SDR and SDG signals were also found to be produced by the avalanche injection of holes across the interface.

Clearly the combination of ESR, SDR, SDG and the non-resonant signals found here offer considerable scope for the investigation of the Si-SiO_2 interface.

Acknowledgement

All figures quoted are from the thesis of Dr. R.L. Vranch.

References

1. Poindexter E.H., Caplan P.J., Johnson N.M., Biegelsen D.K., Mayer M.D. and Chang S.T. in "Insulating films on semiconductors" Ed. J.F. Verwey and D.R. Wolters, 1983, North-Holland, 24; also Poindexter E.H., Ahlstrom E.R. and Caplan P.J. in "The physics of silicon dioxide and its interfaces" Ed. S.T. Pantelides, 1978 Pergamon, 227.

2. Brower K.L., Appl. Phys. Lett. 1983, 43, 1111.

3. Kaplan D., Solomon I and Mott N.F., J.de Physique Lett., 1978 39 L51.

4. Poindexter E.H., Gerrardi G.J., Reuckel M.E., Caplan P.J., Johnson N.M. and Biegelsen D.K. 1984, J. Appl. Phys. 1984 56, 10.

5. Caplan P.J., Poindexter E.H., Deal B.E. and Razouk R.R., Surface Science 1976, 54, 33.

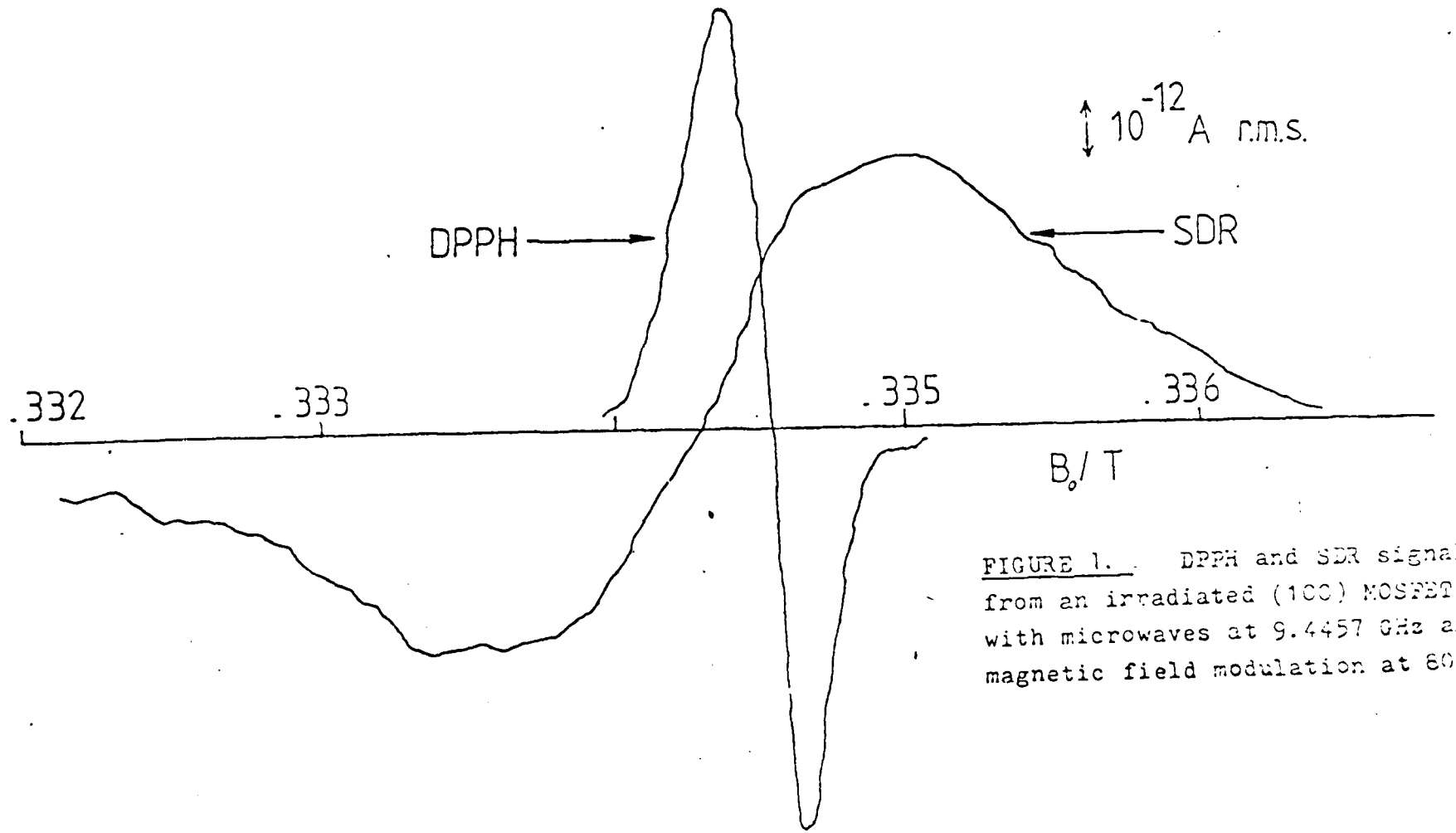

FIGURE 1. DPPH and SDR signals from an irradiated (100) MOSFET with microwaves at 9.4457 GHz and magnetic field modulation at 800 Hz.

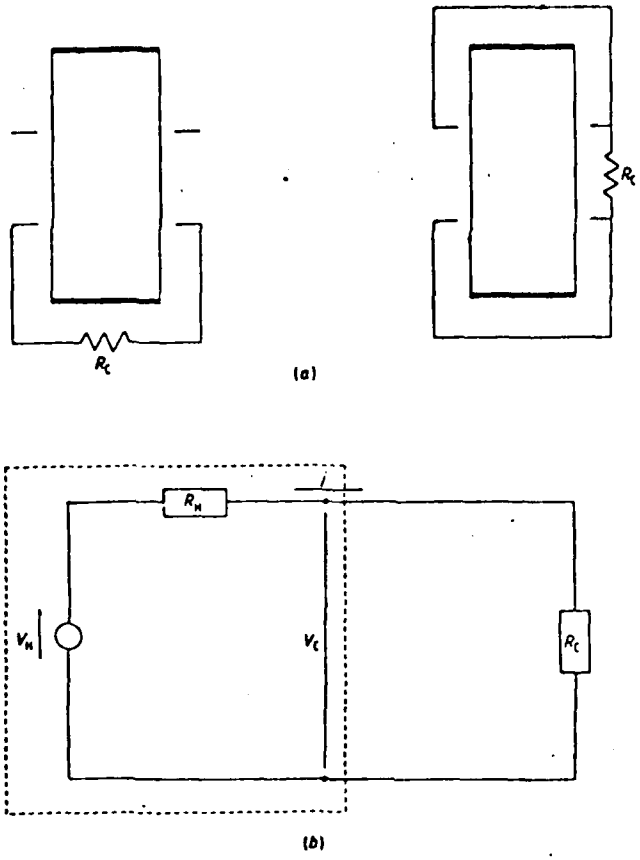

Figure 3. (*a*) The two connected geometries considered; in each case R_C was known to within 1 part in 10^3. (*b*) Thevenin source equivalent of opposite inversion layer contacts.

two geometries on which detailed measurements have been made (figure 3(*a*)), and treat the problem in terms of a Thevenin equivalent circuit.

In a quantised regime let us model contacts between which a Hall voltage is observed by a source having impedance R_H and output voltage $V_H = jR_H$, where j is the current passing (see figure 3(*b*); $R_H = h/ie^2$). When connected via resistance R_C, the voltage appearing externally across the contacts will be

$$V_C = V_H\left(\frac{R_C}{R_C + R_H}\right).$$

The voltage appearing between any two contacts through which all the current flows must be jR_H if a quantised Hall resistance is to be measured. Thus, allowing for the sense of potential drops, the total voltage appearing between source and drain when current j flows will be

$$V_{sd} = V_H + \left[V_H - V_H\left(\frac{R_C}{R_C + R_H}\right)\right] \qquad \text{for geometry (i)}$$

under these circumstances (Tsui *et al* 1983), all resistive effects occur where current enters or leaves a contact. If the current path in the device may be altered so as to enter and leave the inversion layer at several contacts, either in series or parallel, then it ought to be possible to tailor the two-terminal conductance to be any rational fraction of the quantised value in a quantised region. Such modification of the current path may readily be achieved by electrically connecting selected inversion layer contacts, the new current

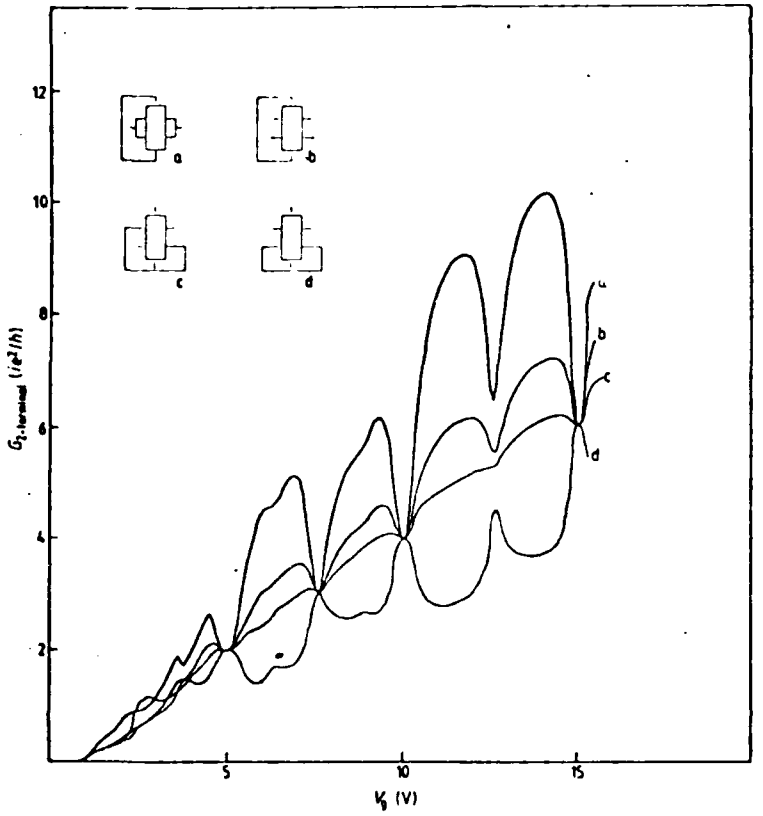

Figure 2. Two-terminal conductance of Si MOS Hall bar with cross-connected inversion layer contacts, as marked (see device sketch for geometry). Connections chosen to give $G = ie^2/h$; the dependence of two-terminal conductance on current path away from the quantised regime is clearly seen.

path then being determined by the imposed equipotentials and the sense of the magnetic field. The results of such a technique for various connections, chosen to yield conductance $ie^2/2h$, are shown in figure 2; the strong influence of current path on conductance away from the quantised regime is clearly seen here. Such results compare with those obtained recently by other workers (Syphers *et al* 1984).

The outstanding problem is, then, what effect the resistance of the contact interconnections has on the accuracy of the quantised resistance values obtained. We consider

overall dimensions 400 μm × 50 μm, were used (these devices were identical to those used by von Klitzing *et al*). Measurements of the two-terminal conductance between various contacts (as labelled) were made in a magnetic field $B = 7.5$ T at a temperature $T = 1.3$ K (figure 1). The plateaus seen at $i = 4$, 8 and 12 show conductances of ie^2/h to within a few parts in 10^4. Concurrent measurement of the four-terminal resistance (as

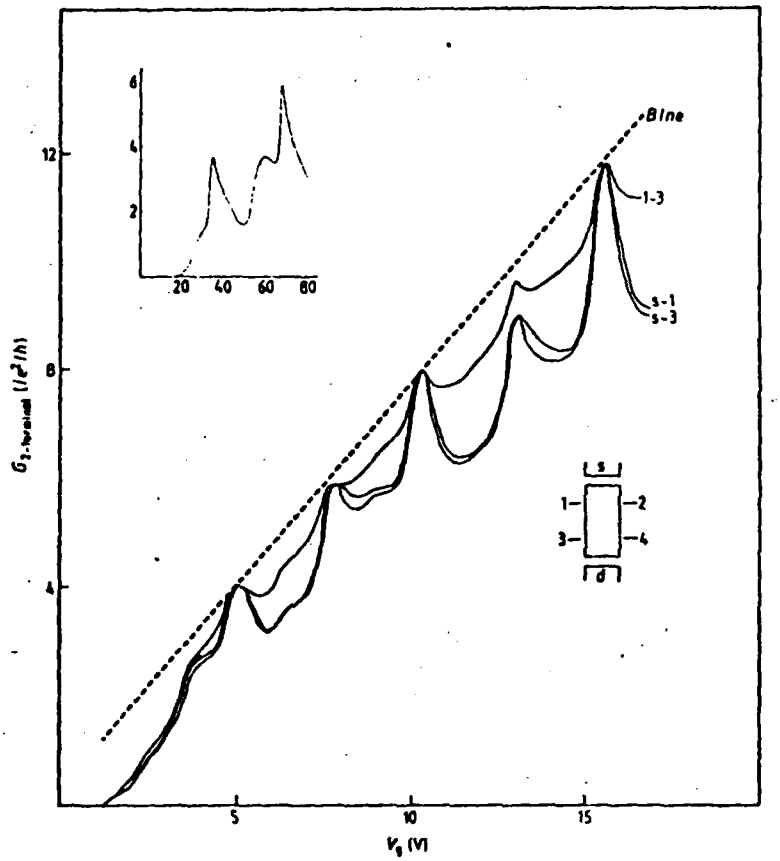

Figure 1. Two-terminal conductance of Si MOS Hall bar ($B = 7.5$ T, $T = 1.3$ K), terminal pairs as marked (see device sketch for terminal designation). Inset is a similar result for a small aspect ratio sample ($W/L = \frac{1}{15}$), which is seen to show plateaus ie^2/h to within a couple of percent.

measured between adjacent Hall probes) showed zeros in the quantised regime, with zero width equal to conductance plateau width to within a few percent. Inset is a preliminary result for a comparable device with much smaller aspect ratio, having overall dimensions 120 μm × 2 μm.

The insensitivity of two-terminal conductance to device aspect ratio in a quantised regime is a consequence of current flow in the inversion layer being without dissipation

J. Phys. C: Solid State Phys.

LETTER TO THE EDITOR

Two-terminal conductance of the quantised Hall resistor

T G Powell†, C C Dean† and M Pepper†‡

† Cavendish Laboratory, University of Cambridge, Madingley Road, Cambridge CB3 0HE, UK

‡ Also at The General Electric Company plc, Hirst Research Centre, East Lane, Wembley, Middlesex, UK

Received 31 January 1984

Abstract. Two-terminal conductance measurements on a two-dimensional inversion layer are shown to give values ie^2/h when E_F lies between Landau sub-bands. Investigation of conductance with resistive connections across the inversion layer shows opposite contacts to behave as a voltage source with characteristic impedance h/ie^2.

In the presence of a magnetic field, the density of states of a two-dimensional electron gas becomes a series of broadened Landau levels, separated in energy by $\hbar\omega_c$. The lifting of spin and valley degeneracies further splits each of these levels into a set of Landau sub-bands (see Ando *et al* 1982 and references therein). Electron scattering is restricted to states within kT of the Fermi level (the Pauli exclusion principle), and so when E_F lies between adjacent Landau bands, or in the region of localised states in the tail of one of the Landau sub-bands, then the rate of scattering in current carrying, extended states below E_F falls to zero. Under these circumstances current is carried either by electrons excited to extended states in the next sub-band above E_F, or by hopping of electrons in the localised states at E_F. Both the diagonal conductivity σ_{xx} and resistivity ρ_{xx} then approach zero with an exponential temperature dependence (Nicholas *et al* 1978, Pepper 1978, Englert and von Klitzing 1978). The off-diagonal resistivity ρ_{xy} takes the value h/ie^2, where i is the number of filled Landau sub-bands (including spin and valley splittings). This quantisation of the Hall resistance was first noted by von Klitzing *et al* (1980), although it was clearly present in the results of earlier work (see Kawaji 1978 for a review).

Wakabayashi and Kawaji (1978, 1980) further noted that when σ_{xx} and ρ_{xx} tend to zero, the Hall voltage becomes equal to the source–drain voltage. This result is exactly analogous to that of Fang and Stiles (1983), who report that any two-terminal measurement of the resistance of a two-dimensional electron system yields, when E_F lies between Landau sub-bands, a quantised value h/ie^2 *irrespective of contact geometry*, while resistance away from such a quantised region is dependent on the aspect ratio of the measurement.

We report measurements of the two-terminal conductance of a MOS inversion layer, which shows quantised values of conductance ie^2/h when the Fermi level lies between Landau bands, a result analogous to that for resistance measurements. Conventional, p-type substrate, Si(100) Hall bar devices, having an oxide thickness of 0.12 μm and

0022-3719/84/130359 + 06 $02.25

the excitation energies. The role of impurities and defects can be significant as the PC curve at low energies can be dominated by their presence.

This work was supported by SERC and in part by the European Research Office of the US Army. P W A McIlroy acknowledges an SERC research studentship.

References

Binnig G, Rohrer H, Gerber Ch and Weibel E 1982 *Appl. Phys. Lett.* **40** 178
Inkson J C 1972 *J. Phys. C: Solid State Phys.* **5** 2599
Jansen A G M, Van Gelder A P and Wyder P 1980 *J. Phys. C: Solid State Phys.* **13** 6073
Leung K M 1984 *Solid State Commun.* **50** 449
Pepper M 1980 *J. Phys. C: Solid State Phys.* **13** L709
Powell C J and Swan J B 1959 **115** 689
Raether H 1980 *Excitation of Plasmons and Interband Transitions by Electrons* (Berlin: Springer)

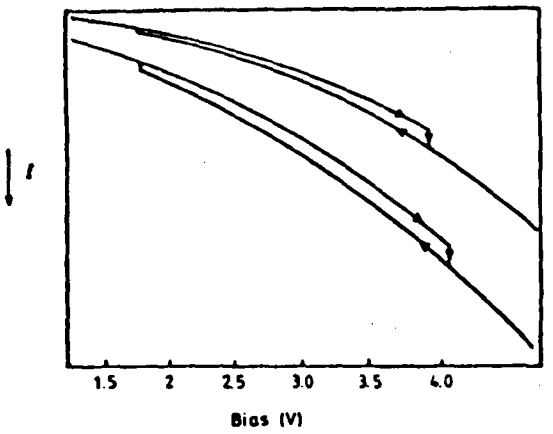

Figure 5. Hysteresis loop in the *I–V* characteristic of the Ag:Si junction; the lower curve shows the shift in the characteristic with time.

In order to investigate the role of plasmon excitations we fabricated Ag:Si contacts which could exploit a radiative surface plasmon at 3.78 eV (Raether 1980). Thirteen Ag contacts were measured in all, twelve of these showed no effect at bias of voltages up to 4.5 eV but one showed similar effects to the first aluminium contact. As the voltage was increased from zero the current increased monotonically up to 500 μA at 3.7 V, whereupon it suddenly increased to 560 μA. If the voltage was then decreased the current traced out a hysteresis loop dropping abruptly to the low current value at approximately 1.8 V, whereafter the loop could be traced out again by increasing the voltage a second time. (Reversing the sweep direction between 1.8 and 3.7 V caused the current to retrace its path; no subsidiary loops were observed). As time passed both the lower and upper limits of this loop shifted to higher bias voltages, as shown in figure 5. When the junction bias was relaxed to +3.3 V for 16 h, the current remained in the 'high' state, with a change of current of less than 1%, indicating that the hysteresis loop was stable over long periods of time. However, a short pulse of length less than 10 μs and amplitude sufficient to raise the bias above four volts would switch the contact from its 'low current' to a 'high' current state.

The junction voltage required for switching into the high state is close to that expected for plasmon-induced switching. Presumably, as with Al junctions, the strong increase in current arises from electrons losing energy rapidly and dropping into a higher mobility state. The strong electron–plasmon coupling ensures that this is a very fast and efficient process.

It is not clear why the hysteresis loop is present below the plasmon energy as, at first sight, the process should switch off at this energy. Possibly a change in current injection pattern, or lines of force, occurs at this energy and is frozen in, only relaxing at a much lower voltage.

In conclusion, we have observed resonant structure in d^2I/dV^2 and current switching voltages close to the Ag and Al surface plasmon energies. Extreme difficulty has been found in fabricating junctions which show these effects, possibly arising from heat dissipation if the resistance is too low and the geometrical shape of the junction altering

the $m = 3$ and $m = 1$ modes. We note that Leung (1984) has found that incorporation of size quantisation results in a mode at ≈9.3–9.2 eV, as found here, for excitations in small Al particles.

Over a period of half a day the 9.3 peak in d^2I/dV^2 changed positions towards higher voltages, intensified and split into twin peaks at 10.4 and 10.54 V (figure 3a), after which the 10.54 V peak diminished leaving only the 10.4 V peak. If the peak at 9.3 V is interpreted as a Mie mode, then this shift in peak energy corresponds to the annealing of the end of the filament from spherical ($a < 130$ Å) to a more planar ($a > 130$ Å) geometry. The fact that the observed energy of 10.4 V corresponds closely to the surface plasmon energy of 10.3 V at the metal–vacuum interface confirms the earlier postulate that the electrons are tunnelling through a thin vacuum gap between the metal and the semiconductor.

Finally, the structure dropped in energy to 10.1 V and subsidiary peaks appeared at 9.9 V and 9.7 V, assuming the shape of resonances (figure 3(*b*)). At this point, the bias circuit started to oscillate at a frequency given by the time constant of the low-pass filter used to eliminate noise. The oscillation was found to be due to a negative resistance in the microcontact and appeared at ≈10 V, was largest around 10.9 V and disappeared above 11.4 V. A circuit consisting of only a battery, a 1 kΩ resistor in series with the contact and a 6.8 μF capacitor in parallel with the contact oscillated at just under 1 Hz, with amplitude of 0.75 mV; changing the capacitor to 32 μF increased the period from 1.1 to 2.1 s. The waveforms of these oscillations are shown in figure 4. The mechanism for the oscillations may be a current switching as found before or a differential negative resistance not observable in the DC characteristic.

As the oscillations observed in this second device are attributable to Al surface plasmons, then plasmons may account for the observed switching in current from 3.8 to 4.2 mA in the first device, although we cannot present an explanation for the higher value of voltage (11.9 V). Possibly this energy may be due to a lowering of the bulk plasmon energy in very small aluminium particles; a geometrical effect seems the most probable cause, or a voltage drop across another part of the system necessitating an applied voltage slightly in excess of the plasmon energy.

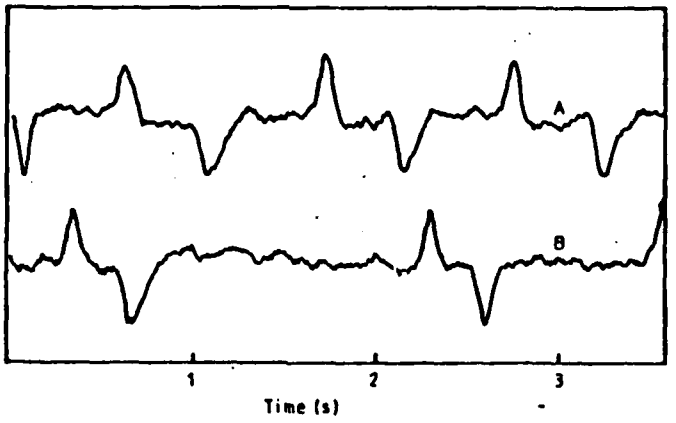

Figure 4. Oscillations set up by the high-voltage differential negative resistance showing the waveform for two different *RC* time constants : (*a*) $C = 6.8$ μF; (*b*) $C = 32$ μF.

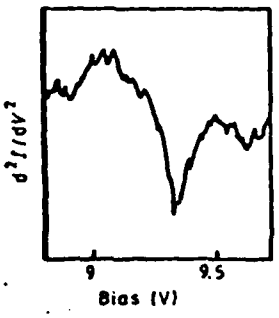

Figure 2. Expanded plot of the resonance at +9.3 V.

surface is placed next to a dielectric medium of relative dielectric constant ε then the surface plasmon energy is $\hbar\omega(1+\varepsilon)^{-1/2}$ (Inkson 1972), and the presence of SiO_2 next to the aluminium reduces the energy of an Al:SiO_2 interface plasmon to 6.9 eV. Structure was not observed at this energy although there was a noticeable increase in noise. If the d^2I/dV^2 maximum is due to an Al plasmon it cannot be at an Al:SiO_2 interface, but must be at an Al: vacuum interface. Spheres of metal of radius $a < c/\omega$ (c is the velocity of light and ω is the frequency of the bulk plasmon) can exhibit plasma oscillations at frequencies of $\omega(2+1/m)^{-1/2}$ (Mie modes), where m is an integer (Raether 1980). Values of a of the order of 100 Å will be less than c/ω and it is possible that such a mode at the end of the metallic filament could give rise to the peak in d^2I/dV^2 observed at 9.3 V. For a normal surface plasmon at 10.3 eV, i.e. $\omega/\sqrt{2}$, the 9.3 V structure corresponds to $\omega(2+1/m)^{-1/2}$ where $m = 2$; the weaker structure at 9.6 V and 8.8 V could be

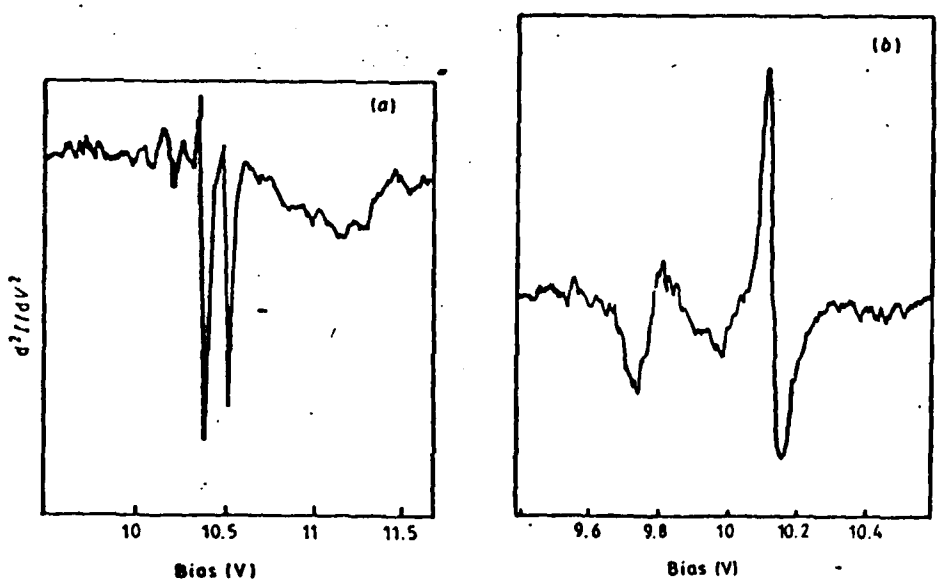

Figure 3. (*a*) High-voltage peaks in the junction spectrum after half a day showing peaks at 10.4 and 10.53 V, and finally (*b*) 9.8 and 10.1 V.

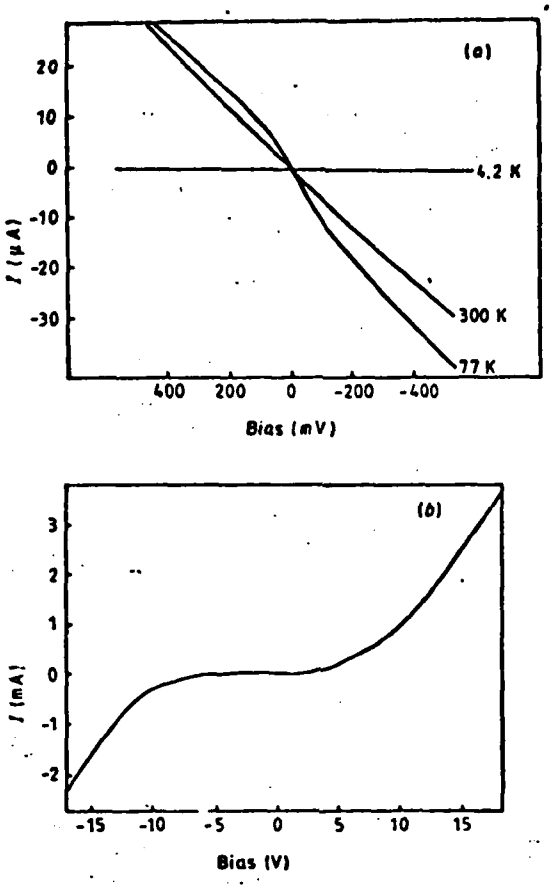

Figure 1. (*a*) Anomalous temperature dependence of the *I–V* characteristic of the Al:Si *junction* discussed in the text. (*b*) The *I–V* characteristic of the junction at 4.2 K.

However, a second Al:Si contact was also found to be stable to high voltages. This contact was noteworthy as it showed a greater current at 77 K than at 300 K, but a much smaller current at 4.2 K (Figure 1(*a*)). The *I–V* characteristic at 4.2 K is illustrated in figure 1(*b*), and a logarithmic plot of this current against voltage indicates that the barrier height φ is ≈ 2 eV, so that the electrons are tunnelling either via the SiO_2, or via a small vacuum gap between the Al and the Si, caused by the contraction of the aluminium filament. A possible explanation for the drop in current at 4.2 K may be differential contraction of the Al filament. The PC spectrum of this device showed a number of features between -5 and $+5$ V. Since neither silicon nor aluminium have any sharp features in their band structure in the range 0 to 5 eV, and the energies and widths of the peaks changed with time, it is clear that they cannot be attributed to interband scattering in Al or Si. Also their energies are too low for plasma oscillations in the Al or the Si to be their origin. There was a d^2I/dV^2 maximum at +9.3, which may be caused by excitation of aluminium surface plasmons (figure 2). Aluminium has a bulk plasmon at 15.3 eV and a surface plasmon at 10.3 eV (Powell and Swan 1959). When the aluminium

LETTER TO THE EDITOR

Non-linearities and electron–plasmon coupling in metal–semiconductor point contacts

P W A McIlroy† and M Pepper†‡
† Cavendish Laboratory, University of Cambridge, Madingley Road, Cambridge CB3 0HE, UK
‡ GEC Hirst Research Centre, East Lane, Wembley, Middlesex, UK

Received 18 October 1984

Abstract. We have investigated the current–voltage characteristics of Al:Si and Ag:Si point contacts in the region of energy corresponding to plasmon excitation. We present results showing resonant structure in d^2I/dV^2 close to the Al surface plasmon energy and bistable switching close to the Al and Ag surface plasmon energies.

Point contact (PC) spectroscopy is now a well established technique for the study of inelastic processes in metal–metal point contacts (Jansen *et al* 1980). However, melting of the contacts limits the useful range of such experiments to energies below a few hundred meV, so that high-energy phenomena such as interband transitions and plasma oscillations cannot be observed. Metal–semiconductor ohmic contacts have much higher ratios of electrical to thermal resistance, and can withstand three or four volts of bias without damage. If there is an oxide barrier between the metal and the silicon, or a vacuum gap (Binnig *et al* 1982), then the bias voltage can be increased to still higher values so that inelastic tunnelling phenomena can be observed at biases in excess of 10 V. In this Letter we report the observation of non-linearities and negative resistance phenomena in aluminium–silicon and silver–silicon point contacts at energies close to the metal–surface plasmon energies. The method of contact formation and derivative measurement was the same as described previously (Pepper 1978), except that the bias circuit was modified to provide a stable sweep over the range −20 to +20 V.

Most of the metal–semiconductor microcontacts we investigated were unstable at bias values above 3 V. However, one silicon–aluminium contact sustained a voltage of 15 V without catastrophic failure. This sample showed a marked singularity in its I–V characteristic at +11.9 V: below this voltage the current increased uniformly up to 3.8 mA, but at 11.9 V (Al positive) the current increased abruptly to 4.2 mA. Above this voltage the current again increased uniformly, up to 8 mA at 15 V bias. This discontinuous rise in current could be attributed to the melting and reforming of the contact due to heating were it not for the fact that the rise in current was reversible: each time the voltage was increased from zero the contact current was the same, always increasing abruptly from 3.8 to 4.2 mA at 11.9 V bias in less than the response time of the chart recorder. Unfortunately this contact catastrophically failed when the voltage was increased above 15 V, and so further measurements could not be performed on it.

0022-3719/85/040087 + 06 $02.25

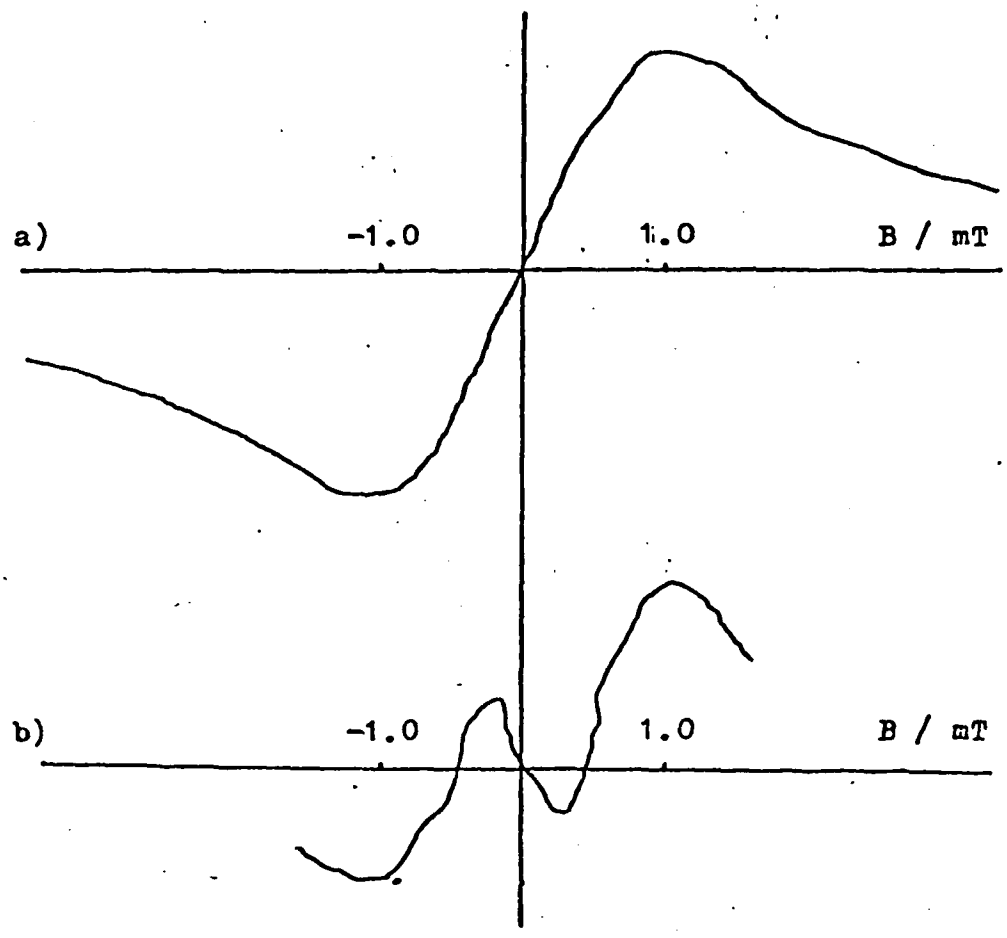

FIGURE 5.

a) A non-resonant SDR signal from a p-channel (111) MOS device with $\underline{B} \perp [111]$ and a modulation field of 1.2 mT ptp (as figure 5.1).

b) A signal recorded under similar conditions to a) but with a modulation field of 0.4 mT ptp and a more sensitive current scale.

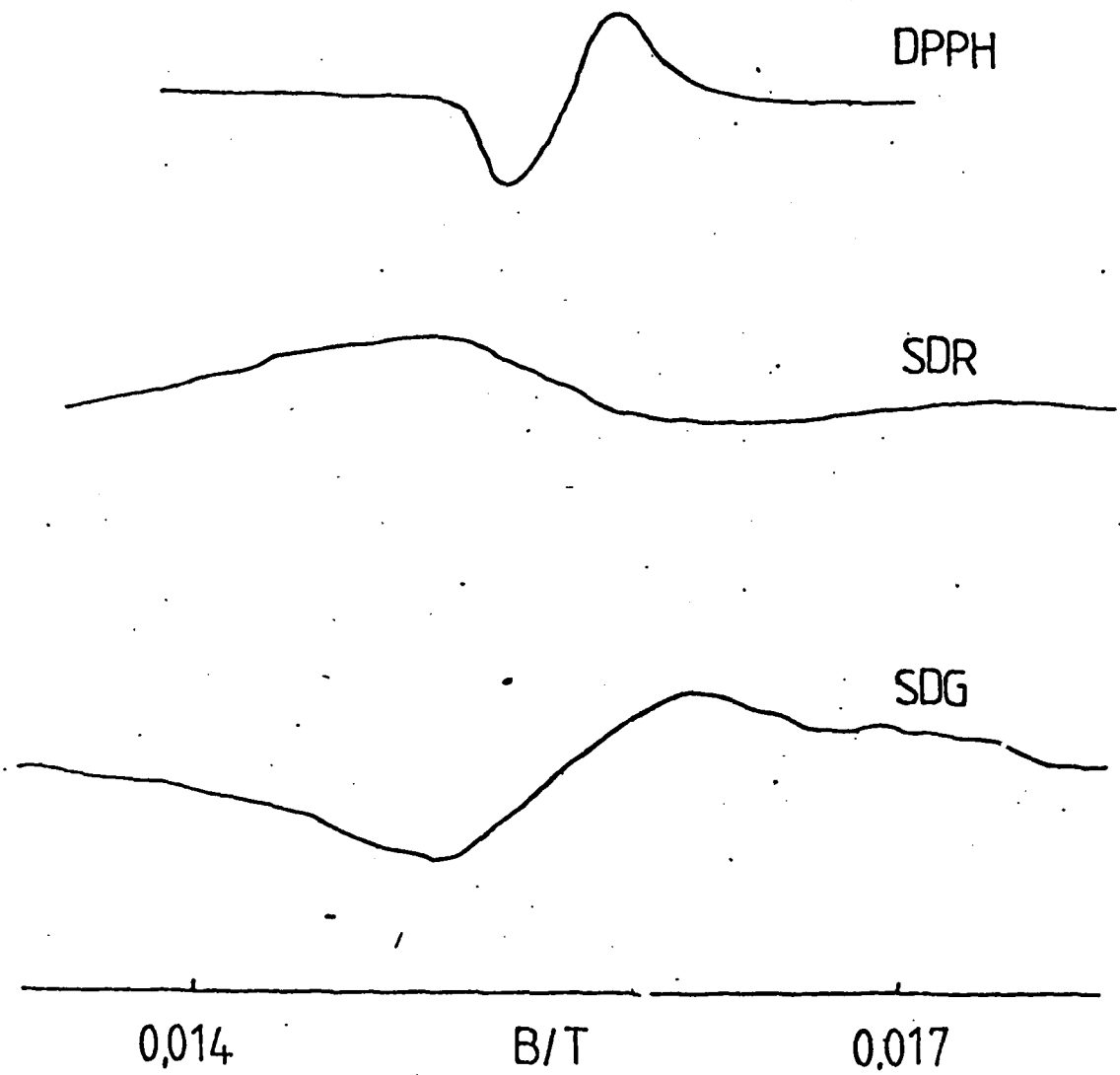

FIGURE 4. Spin resonances at 440 MHz.

SDR: I_{dc} = 20 nA, sensitivity 2×10^{-12} A r.m.s. cm^{-1}

SDG: I_{dc} = -1.0 nA, sensitivity 10^{-13} A r.m.s. cm^{-1}

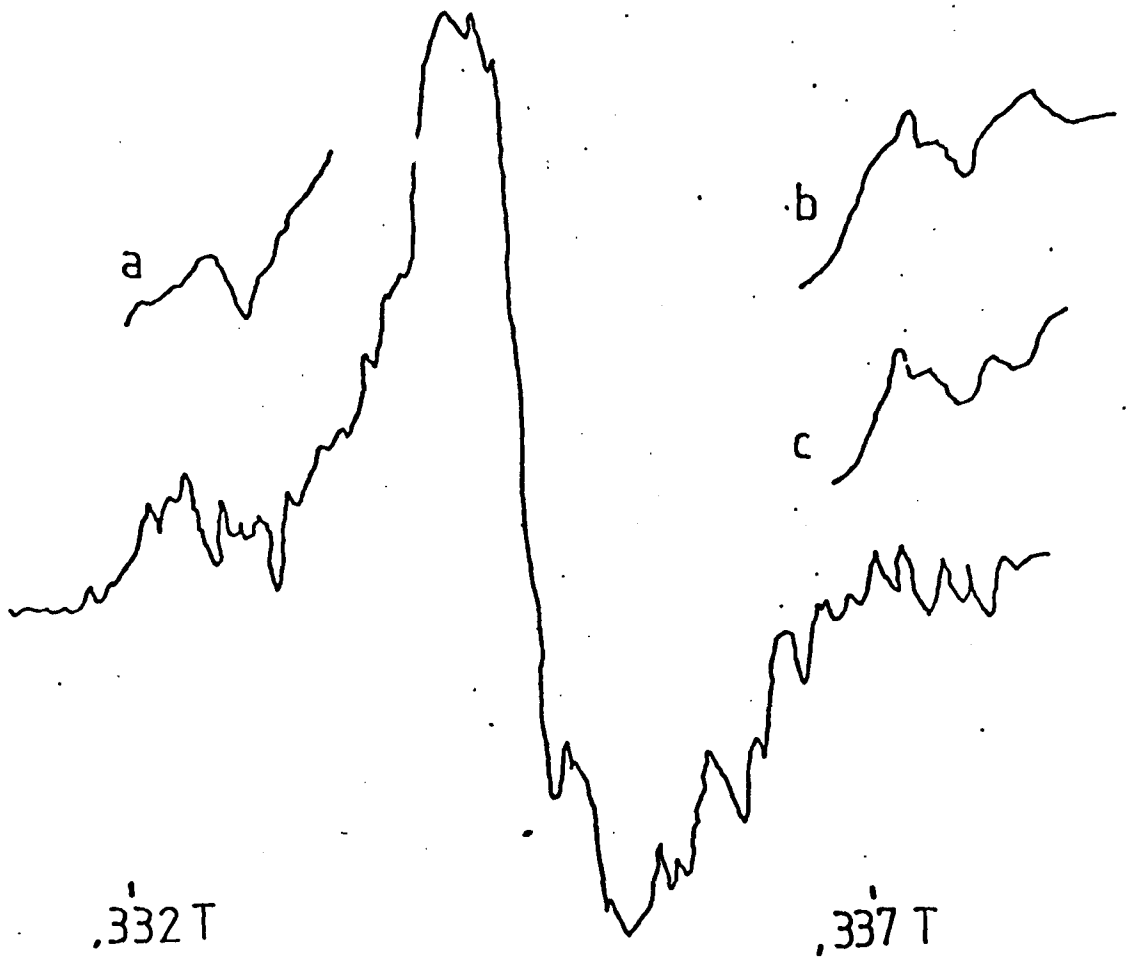

FIGURE 3. An SDG signal from a p-channel (111) MOS device showing small resonances on either side of the main resonance. The traces a, b and c were recorded on the same B_0 scale with twice the sensitivity and a longer lockin amplifier time-constant (10^{-13} A r.m.s. cm^{-1}, 30 s) The microwave frequency was 9.4527 GHz.

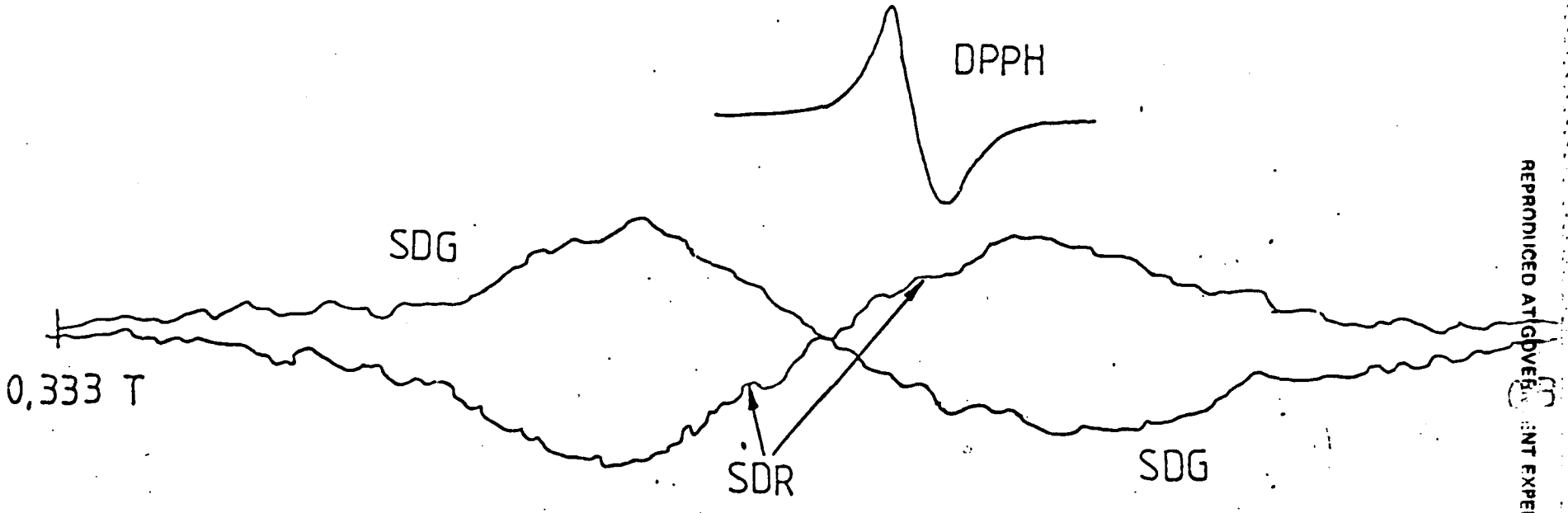

FIGURE 2.

An SDG signal (with I_{dc}= -1.6 nA and 10^{-13} A r.m.s. cm^{-1} vertical scale) and an SDR signal (with I_{dc}= 21 nA and 10^{-12} A r.m.s. cm^{-1} vertical scale). The DPPH signal was recorded with a forward current. The sample was a (100) electron-irradiated MOSFET. V_G was -18 V (to give the maximum surface recombination current).

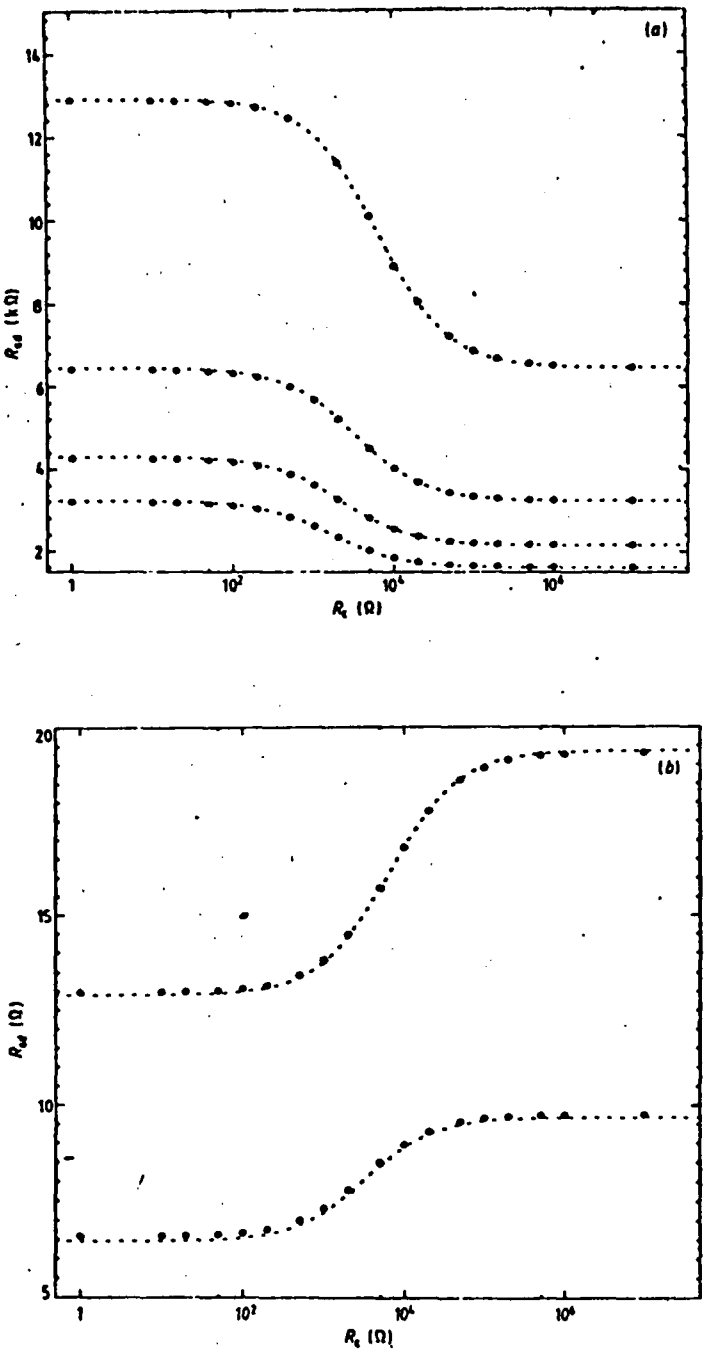

Figure 4. Source–drain resistance for (*a*) geometry (i) and (*b*) geometry (ii), with resistively connected inversion layer contacts ($B = 7.5$ T, $T = 1.2$ K). Data points are as marked with asterisks, the broken curve showing the corresponding values obtained from the theoretical expression.

and

$$V_{sd} = V_H + \left[V_H + V_H\left(\frac{R_C}{R_C + R_H}\right)\right] \qquad \text{for geometry (ii).}$$

The overall source–drain resistance measured in the two cases is then given by

$$R_{sd} = 2R_H\left[1 \pm \frac{1}{2}\left(\frac{R_C}{R_C + R_H}\right)\right]. \tag{1}$$

Measurements of source–drain resistance were made for both geometries, with various values of R_C (figure 4). In each case, values from the above expression are shown for comparison. There is clearly good agreement between experiment and this simple analysis.

Finally we note that, if the analysis is extended to an infinite number of contacts across the device (as geometry i), then the result given is the same as that for a Corbino geometry device.

We are grateful for many useful discussions with Professor P J Stiles, Dr A P Long and Dr H W Myron (University of Nijmegen, Holland). This work was supported by the SERC, and T G Powell and C C Dean acknowledge the support of SERC research studentships. Partial support also came from the European Research office of the US Army.

References

Ando T, Fowler A B and Stern F 1982 *Rev. Mod. Phys.* **54** 437
Englert T and von Klitzing K 1978 *Surf. Science* **73** 70
Fang F F and Stiles P J 1983 *Phys. Rev.* B**27** 6487
Kawaji S 1978 *Surf. Science* **73** 46
von Klitzing K, Dorda G and Pepper M 1980 *Phys. Rev. Lett.* **45** 494
Nicholas R J, Stradling R A, Askenazy S, Perrier P and Portal J C 1978 *Surf. Sci.* **73** 106
Pepper M 1978 *Phil. Mag.* B**37** 83–95
Syphers D A, Fang F F and Stiles P J 1984 *Surf. Sci.* to be published
Tsui D C, Stormer H L and Gossard A C 1983 *Phys. Rev.* B**25** 1405
Wakabayashi J and Kawaji S 1978 *J. Phys. Soc. Japan* **44** 1839
—— 1980 *Surf. Sci.* **98** 299

Frequency Dependent Magnetoconductance Quantisation in 2D Systems - a Disorder Effect

by

T G Powell*, R Newbury*, A P Long$, C McFadden*, H W Myron+ and M Pepper*$

* The Cavendish Laboratory, Madingley Road, Cambridge CB3 OHE, UK

$ The General Electric Company plc, Hirst Research Centre, East Lane, Wembley, Middlesex, UK

+ High Field Magnet Laboratory, University of Nijmegen, Nijmegen, The Netherlands.

ABSTRACT

Strong frequency dependence is shown in the quantised magnetoconductance in high mobility silicon MOSFETs, with the loss of integer quantised plateaux and enhancement of fractional quantisation. Fractional plateaux observed are quantised to within 5%, which is within experimental accuracy. The frequency at which the onset of these phenomena is observed is shown to be dependent upon sample length and Landau level filling factor. The results are similar to those previously obtained using low mobility GaAs heterostructures, though in the highest mobility cases no effect is seen up to 50 MHz. The roles of sample length and disorder are discussed.

Fractional quantisation of the Hall resistance in a two-dimensional system was first observed in high mobility GaAs-AlGaAs heterojunctions at temperatures below 1 K (Tsui *et al* 1982), DC measurement techniques being employed. Subsequent work on heterostructures (Stormer *et al* 1983 , Chang *et al* 1984) has indicated that only non-integer rational fractions occur, though no general rule indicating which fractions show greatest stability has been found. Since then, structure at fractional Landau level filling factors has also been observed in highest mobility ($\mu \approx 4.0$ m^2/Vs) silicon MOSFETs (Pudalov *et al* 1984), confirming the effect to be a general characteristic of two-dimensional systems, and not restricted to heterostructures. In all these cases, strong integer quantisation is observed concurrent with the observation of the fractional effect.

In lower mobility heterostructures and silicon MOSFETs, or at higher temperatures (Chang *et al* 1983), fractional quantisation is not generally seen. Recently, however, we have shown that increase in signal frequency causes a reduction in size and eventual loss of integer plateaux, which has been attributed to the effective delocalisation of electrons by frequency. As integer quantisation is lost in this way, fractional quantisation may be observed (Long *et al* 1984, McFadden *et al* 1984). The loss of integer plateaux appears to be a prerequisite for the observation of fractional quantisation, and even with DC measurements greatly reduced integer plateaux widths are observed when the fractional quantum Hall effect is seen (Paalanen *et al* 1984). In the case of silicon, measurement of σ_{xx} in Corbino geometry devices shows that the loss of integer quantisation is accompanied by a narrowing of the zero conductivity region which occurs when σ_{xy} becomes quantised.

We report high frequency measurements on silicon MOSFETs at 1.4 K and in a magnetic field of 20 Tesla. Standard metal gate, p-type substrate Si(100) Hall bars were used, having oxide thickness 0.405 μm, and 4.2 K mobility of 1.5-2.0 m^2/Vs. High frequency lock-in techniques were

employed, monitoring the in-phase signal component having adjusted the phase. Simultaneous measurement of the computed vector magnitude enabled us to ensure that the phase did not change as the sample impedance altered. Two-terminal conductance measurements were made, exploiting the quantised magnetoresisitance (Fang and Stiles 1983, Powell *et al* 1984). Frequencies between 500kHz and 45MHz were used, signal losses at the highest frequencies being minimised by correctly terminating the coaxial lines at the sample.

Two basic Hall bar configurations were available: by pairing opposite Hall probes to act as an effective drain, two-terminal measurements could be made on samples ranging in length from 150 μm to 2000 μm (figure 1). Conductance values shown are derived from the nominal instrument calibration; no corrections have been made for cable losses or similar effects. The conductance seen when the device shows very low two-terminal conductance (V_g<5 volts) may be assumed to be zero, and the data is shown with an arbitrary offset in the y-axis. Landau level filling factor, i_L, is calculated from the known oxide thickness and threshold voltage.

Results on the longest Hall bar, 2000 μm in length (figure 2a), show a strong frequency dependence even as low as 1MHz. A feature is clearly developing at i_L=4/5 between 500 kHz and 2 MHz, and the plateau at i_L=1 is completely destroyed by 4 MHz. The flatness of the 4/5 plateau is more clearly seen on expanding the x-axis (figure 2b): its conductance (compared to the i_L=2 plateau, which has remained quantised) is within 5% of $4/5\sigma_H$ (where $\sigma_H=e^2/h$), which is within experimental accuracy. Further features are seen to develop at i_L=5/3 with a frequency of 4 MHz, and at i_L=8/3 and 11/3 on reaching 8 MHz. Note also the loss of i_L=3 occuring at 10 MHz (the feature is absent by 12 MHz)

At higher frequenies still the accuracy of the fractional quantisation and the flatness of these plateaux is lost, the conductance actually rising above the fractional values. This effect is similar in nature to the

destruction of integer quantisation at lower frequencies, though this need not suggest that the mechanism is the same.

On truncating the Hall bar to give a sample having effective length 800 μm, the same essential features as in the previous case are seen - i.e. progressive loss of the integer quantised plateaux, concurrent with the development of features at fractional filling factors (figure 3a). As in the first case, the onset of these effects occurs at lower frequencies with lower filling factor. However, it is quite clear that the onset frequency at which the phenomena appear is considerably increased. The loss of i_L=1, for example, occurs over a fairly narrow frequency range around 12 MHz (figure 3b), as compared to 4 MHz previously. The rapidity with which the plateau is lost in this case is quite striking.

The same trend of increasing onset frequency with decreasing sample length is also seen in results from the shorter, 430μm long Hall bar (figure 4), and in those obtained on truncating this sample to an effective length of 150 μm (figure 5). Indeed, in the latter case little effect is seen with frequency even above 16 MHz, though cable lossess have become apparent by 30 MHz. It is still clear that the phenomena are seen first at lower Landau level filling factor, and in the case of the shorter samples no significant effects are seen above i_L=2.

Two further points may be noted about the results shown. Firstly, above i_L=1 the most strongly enhanced fraction is that at 2/3 filling of each Landau level. Secondly, the integer plateaux showing the strongest dependence on frequency are the odd, valley split ones. We can present no explanation for these observations, except to note that the valley splitting is the weakest in the system.

Investigation of GaAs heterostructures gave similar effects to those previously reported (Long *et al* 1984). However, frequency-enhanced fractional quantisation was also observed in gated GaAs-AlGaAs heterojunctions (figure 6). It is clear that direct alteration of carrier

concentration by gating also results in the observation of fractional quantisation with increasing frequency. The results of this work show that the disappearance of integer quantisation and the appearance of fractional quantisation with frequency are common to both silicon and GaAs, and so appear to be a general property of two-dimensional systems.

The original explanation of the effect seen on integer quantisation (Pepper and Wakabayashi 1983) is that electron delocalisation with increasing frequency narrows the region in which σ_{xx} is zero, and hence in which σ_{xy} is fully quantised. In this case, states with localisation length longer than the sample length will already be effectively delocalised, and the onset of a frequency effect would be expected when states having localisation length less than or equal to the sample length become delocalised. This leads to a frequency onset for these phenomena which will be sample length dependent. As the minimum meaningful localisation length is the sample length, then the onset of frequency dependent behaviour marks the onset of the response of states having localisation lengths equal to the sample length. Thus the sample length becomes a useful measure of the length scale of the localisation, and provides a means of relating delocalisation length to frequency.

Appearance of fractional quantisation may be expected as the increasing frequency reduces the overall role of disorder. As in the case of integer quantisation, the fractional plateaux evolve into peaks with further increase in frequency. We have no explanation for the observed rise of these fractional peaks to conductances above the quantised values.

More recently it has been suggested (Joynt 1985) that the loss of integer quantisation is related to the existence of semi-classical states in the sample which may show response at relatively low frequencies. It is proposed that these states may contribute to σ_{xx} at finite frequencies even when they are technically localised. As two-terminal measurements yield $\sigma_{xy}-\alpha\sigma_{xx}$ (where α is a geometry dependent constant), any change in σ_{xx} will

be reflected in the conductance seen. The existence of such states depends upon the disordered potential being smooth on a length scale compared to the magnetic length, and will thus be sample dependent. This theory allows one to account for the observed mobility and Landau level filling factor dependences. No similar theory exists at present for the enhancement of fractional quantisation.

Although in these experiments frequency effects were seen in heterostructures, in higher mobility cases ($\mu \geq 10$ m^2/Vs) the integer plateaux remain flat to very high frequencies, and no frequency-enhancement of fracional quantisation is seen (as has been found in pulsed measurements, Woltjer *et al* 1985). The high degree of lattice and interface perfection in such high mobility heterostructures means that the disordered potential is extremely long-ranged. As a result, trapped states associated with impurity sites will not overlap, and any states which are so localised will have very short localisation lengths (this is analogous to high purity semiconductors, which show very strong localisation at low temperatures). These states will respond only at very high frequencies, and this may account for the failure to observe any frequency effect in very high mobility samples.

It is hoped that further experiments on longer devices will lead to a clearer understanding of the relationship between onset frequency and sample length for these effects.

Acknowledgements

We are grateful for the help of the staff at the high magnetic field laboratory of the University of Nijmegen where these experiments were carried out. This work was supported by the SERC, and T G Powell acknowledges the support of a SERC research studentship. Partial support also came from the European Research office of the US Army.

References

Chang AM, Paalanen MA, Tsui DC, Stormer HL and Hwang JCM 1983 *Phys. Rev.* B28 6133

Chang AM, Berglund P, Tsui DC, Stormer HL and Hwang JCM 1984 *Phys. Rev. Lett.* 53 997

Fang FF and Stiles PJ 1983 *Phys. Rev.* B27 6487

Joynt R 1985 to be published

Long AP, Myron HW and Pepper M 1984 *J. Phys. C: Solid State Phys.* 17 L433

McFadden C, Long AP, Myron HW, Pepper M, Andrews D and Davies GJ 1984 *J. Phys. C: Solid State Phys.* 17 L439

Paalanen MA, Tsui DC, Gossard AC and Hwang JCM 1984 *Solid State Comm.* 50 841

Pepper M and Wakabayashi J 1983 *J. Phys. C: Solid State Phys.* 16 L113

Powell TG, Dean CC and Pepper M 1984 *J Phys C: Solid State Phys.* 17 L359

Pudalov VM and Semenchinskii 1984 *JETP Lett.* 39 170

Stormer HL, Chang A, Tsui DC, Hwang JCM, Gossard AC and Wiegemann W 1983 *Phys. Rev. Lett.* 50 1953

Tsui DC, Stormer HL and Gossard 1982 *Phys. Rev. Lett.* 48 1559

Woltjer R, Mooren J and Wolter J_{A}^{neu} *Solid State Comm.* 53 331

figure 1(a)

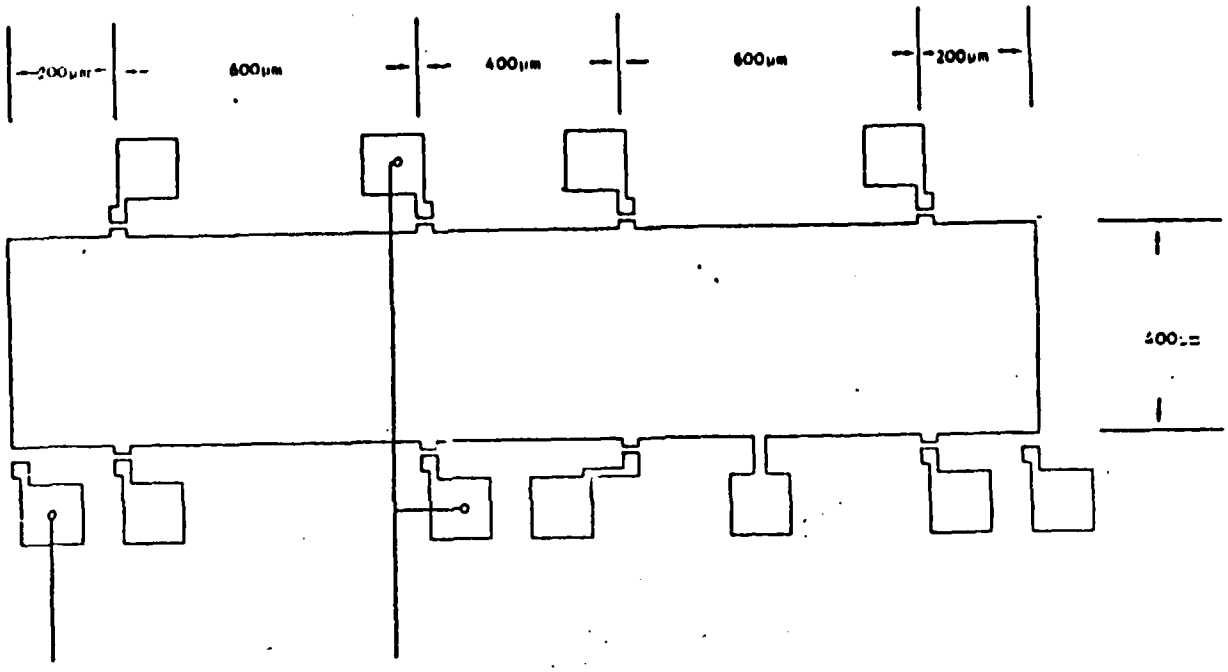

figure 1(b)

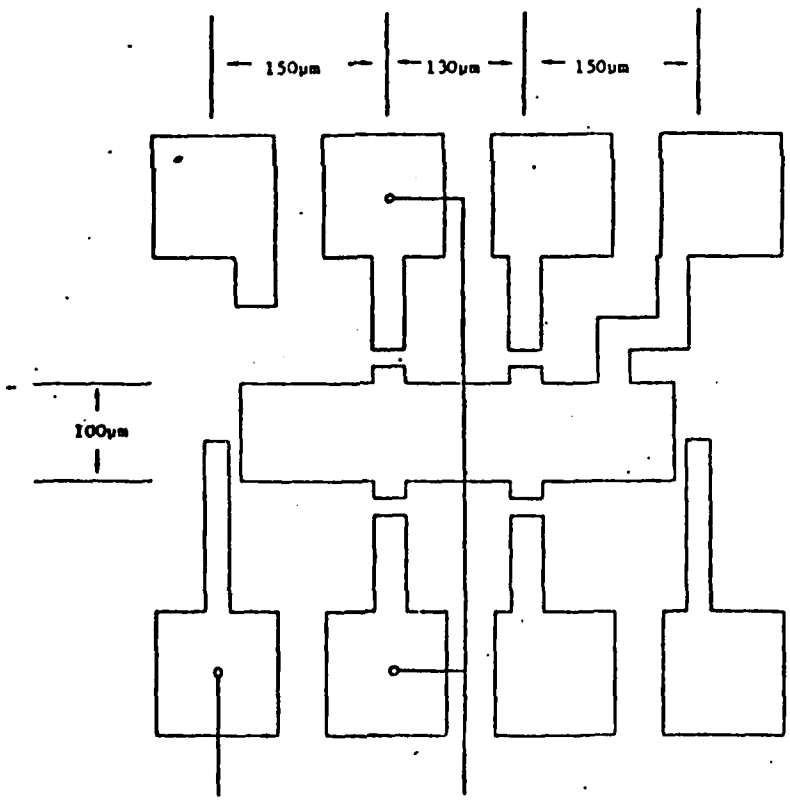

figure 1: the two Hall samples used, showing the Hall probe pairing used to give a truncated sample length; (a) sample lengths 2000 µm and 800 µm , (b) sample lengths 450 µm and 150 µm.

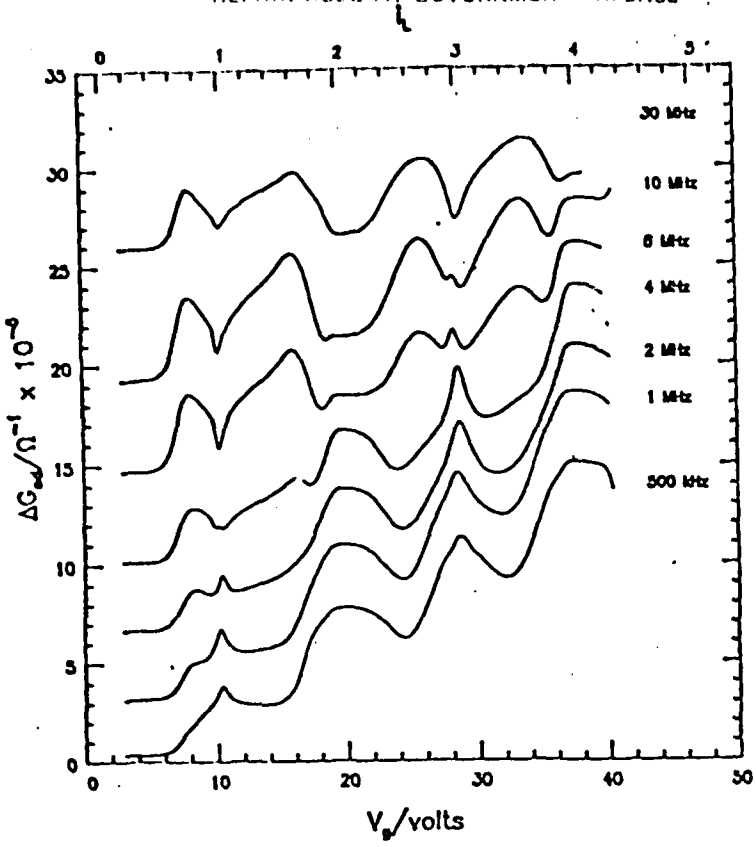

figure 2 (b)

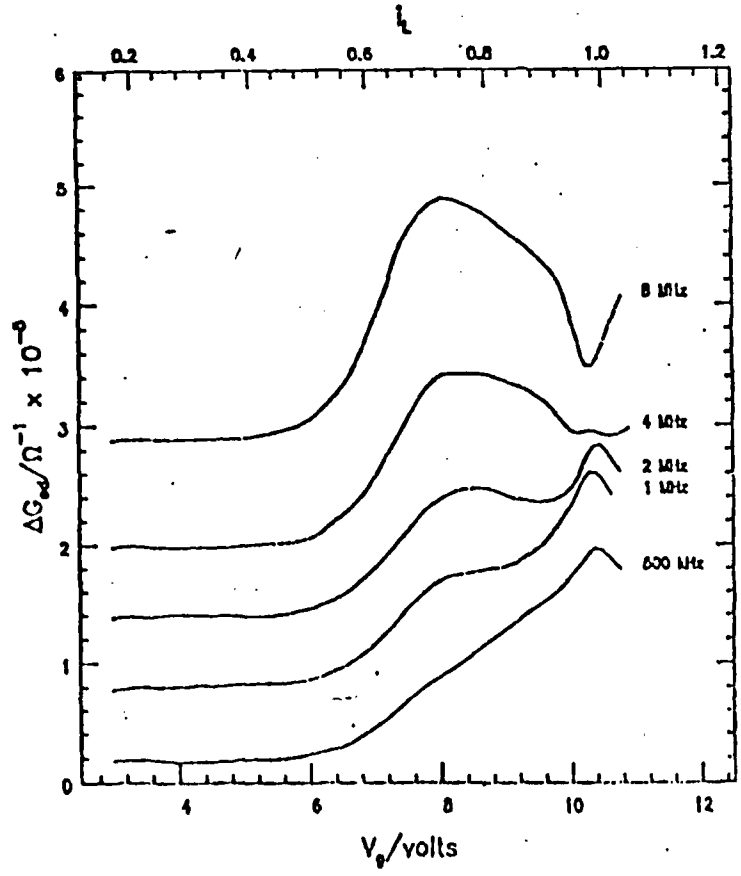

figure 2: frequency behaviour in the longest sample, 2000 μm x 400 μm. At lower frequency, quantisation is accurate within experimental accuracy (σ_H=3.87 x 10^{-5} Ω^{-1}). The flatness of the fraction i_L=4/5 is more clearly seen in (b). B=20.0 T; T=1.4 K; E_{sd}=0.5 Vm^{-1}.

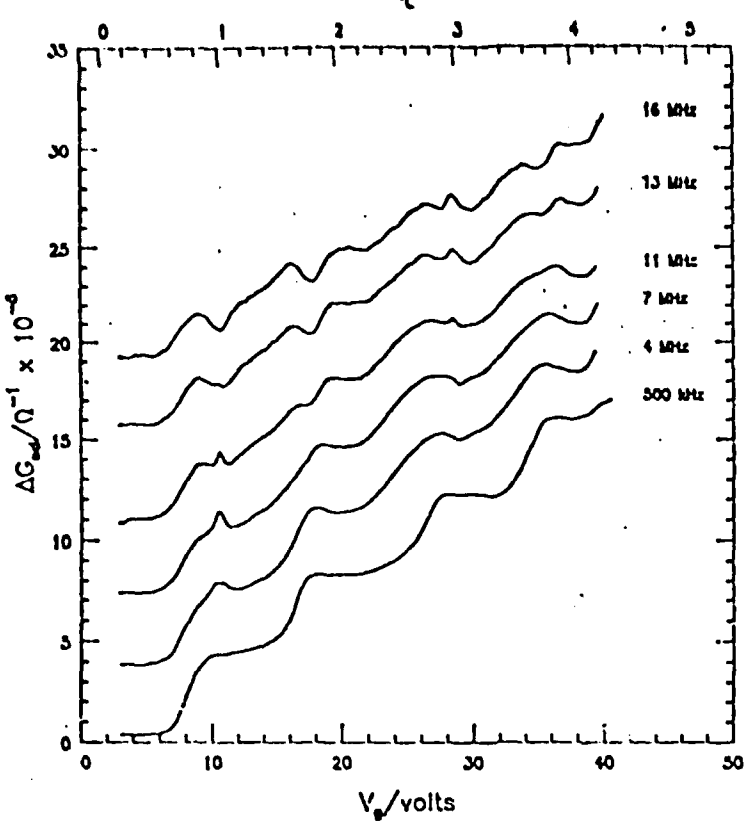

figure 3 (b)

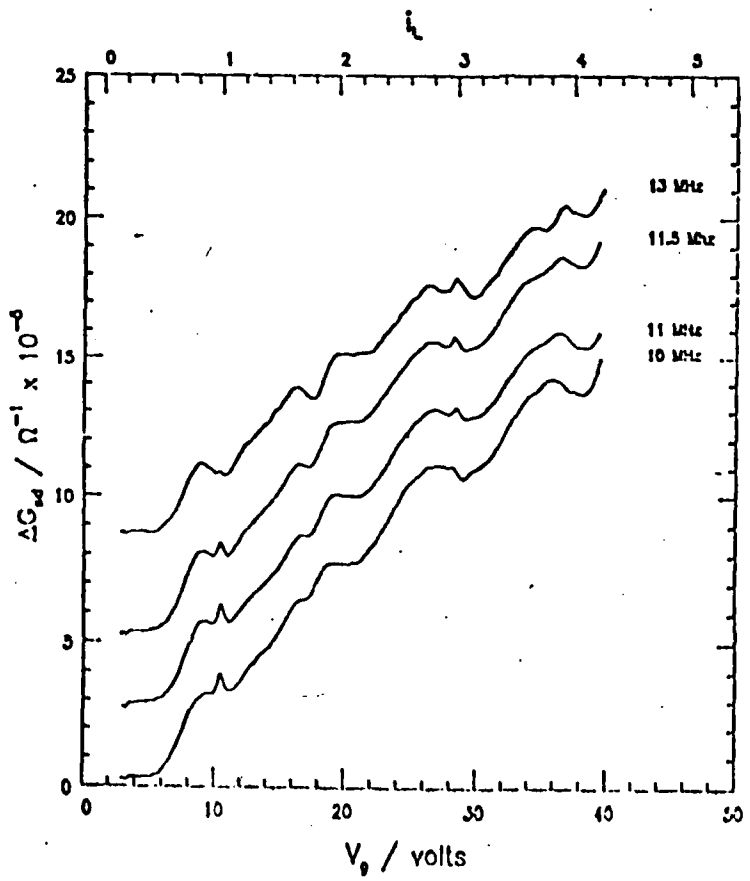

figure 3: truncated long Hall sample, 800 μm x 400 μm. The change in overall shape compared to figure 2 is due to the changed aspect ratio. The rapidity with which $i_p=1$ is lost, between 11.5 MHz and 13 MHz, is clearly seen in (b). B=10.0 T; T=1.8 K; E_{max}=1.0 Vm^{-1}.

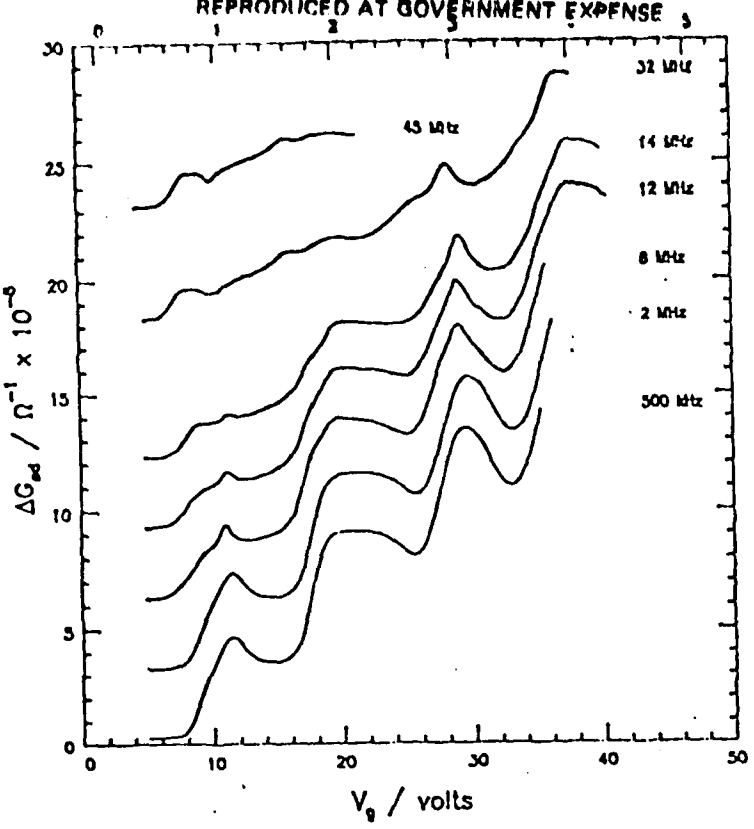

figure 4: frequency behaviour in the shorter sample, 430 μm x 100 μm. Integer quantised features persist to much higher frequencies here. Cable losses are apparent by 32 MHz. B=20.0 T; T=1.4 K; E_{sd}~1.7 Vm^{-1}.

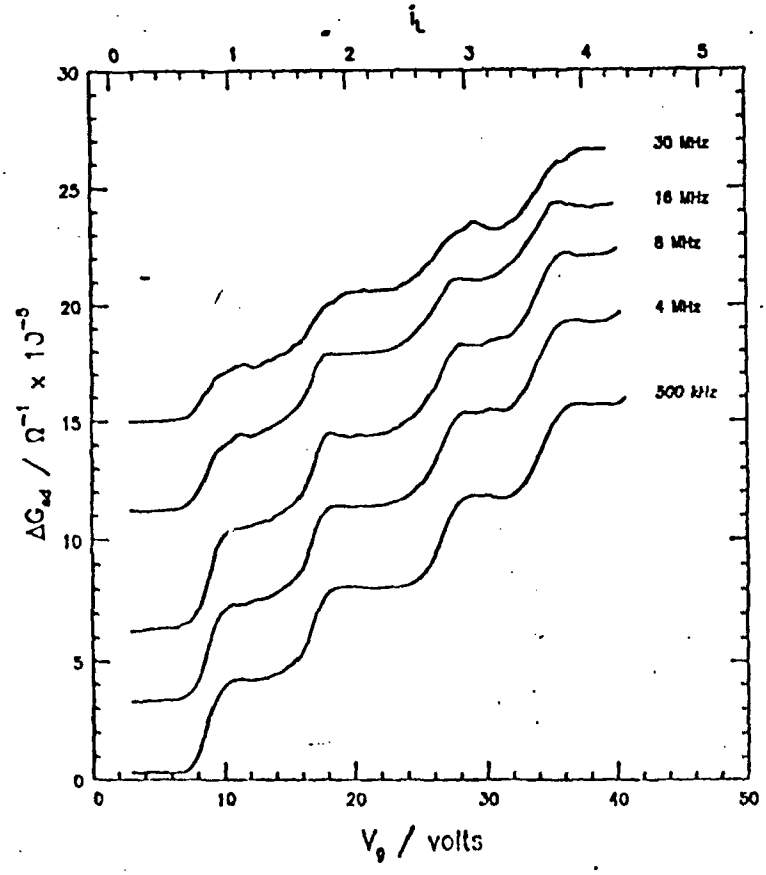

figure 5: truncated short Hall sample, 150 μm x 100 μm. Integer quantisation is fully preserved even at 30 MHz, and no significant enhancement of fractions occurs over the measured range. B=20.0 T; T~1.4 K; E_{sd}~5.3 Vm^{-1}.

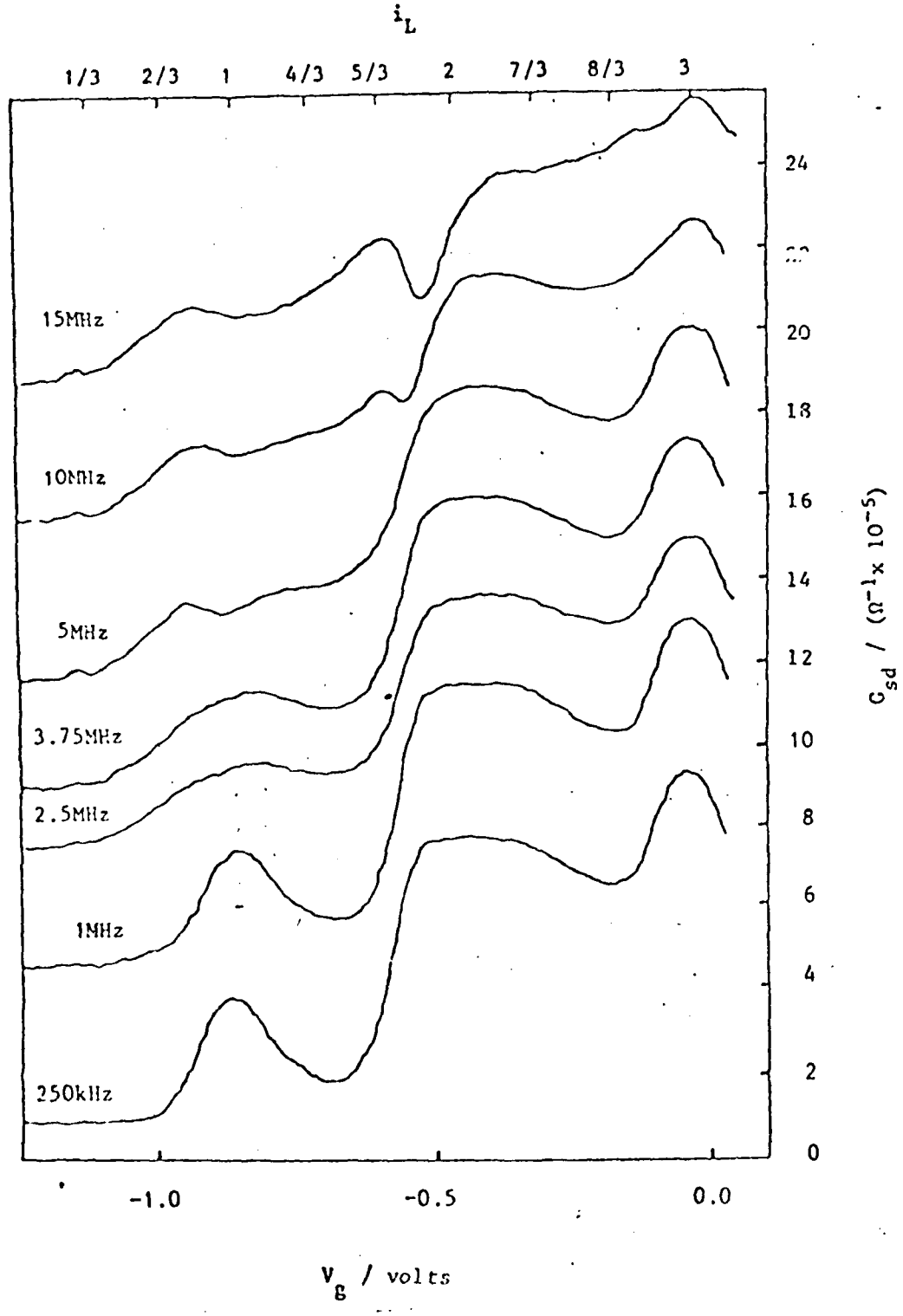

figure 6: frequency-enhancement of fractional quantisation in GaAs-AlGaAs heterojunction. Carrier concentration=4.5 x 10^{15} m^{-2} at V_g=0 volts. B=5.75 T; T~1.4K.

END

FILMED

11-85

DTIC